14th IEA Heat Pump Conference
15-18 May 2023, Chicago, Illinois

Optimization of a Residential Air Source Heat Pump using Refrigerants with GWP <150 for Improved Performance and Reduced Emission

Zhenning Li[a], Samuel F. Yana Motta[a], Bo Shen[a], Hanlong Wan[a]

[a]Oak Ridge National Laboratory, Oak Ridge, TN, 37830 USA

Abstract

Using low-GWP refrigerants can reduce the Green House Gas (GHG) emission of heat pump systems. Heat exchangers and compressors are the key components and have a prominent impact on system performance, significant research is devoted to reducing the cost of the heat exchangers while achieving the same or better system performance with refrigerant charge reduction.

To better understand the environmental impacts of optimized systems with low-GWP refrigerants, Life Cycle Climate Performance (LCCP) evaluation method was used to evaluate the direct and indirect emissions of the system over the course of its lifetime from manufacturing to disposal. The DOE/ORNL Heat Pump Design Model (HPDM) is used to evaluate the performance of heat pumps. Multi-objective optimizations using Particle Swarm Optimization (PSO) algorithm are performed on a 3-ton R410A residential air source heat pump on market. Seven R410A alternatives, i.e., R32, R454B, R454C, R455A, R457A, R1234yf and R1234ze(E) are investigated. The last five fluids have GWP lower than 150.

As a result, 5.5%-12.8% seasonal energy efficiency ratio 2 (SEER2) improvement is achieved, and the optimized systems reduce life cycle CO_2 emission by 8.5%-28.6% with GWP lower than 150 refrigerants. The optimal heat exchangers can fit into the original R410A fan-coil units; therefore, the proposed design method establishes a production and installation path to produce cost-effective low-GWP heat pumps easily accepted by end users.

Selection and/or peer-review under the responsibility of the organizers of the 14th IEA Heat Pump Conference 2023.

Keywords: Low GWP; Heat exchange;, Heat pump; Optimization; LCCP Introduction

1. Introduction

Modern cooling technologies are significant sources of greenhouse gas emissions (GHGs) with total CO_2 equivalent emissions from the HVAC sector accounting for 7.8% of global GHG emissions ([1]. Considering the commitment to reduce the impact of GHGs on climate in the HVAC&R sector, a transition from fluorinated substances to alternative refrigerants with reduced global warming potential (GWP) values is supported by F-gas Regulation ([2], the Montreal Protocol with the Kigali Amendment [3] of which 146 countries have not ratified, and the Paris Agreement [4] and the US AIM ACT. The requirements as set forth by the F-gas Regulation banned the use of refrigerants with a GWP of 2500 or greater for high refrigerant charge stationary HVAC equipment in 2020. Beginning in 2022, a GWP limit of 150 has been set for multi-circuit cascade

systems for commercial use with a nominal capacity of 40 kW or more, and for 2025, the GWP limit for single split AC on the European Union (EU) market is set as 750. This ban will not permit the use of R410A (2088 as GWP value) in small charge system applications. In this regard, much research has been conducted to find alternative low-GWP refrigerants.

Reducing the environmental impacts of HVAC&R systems has been an important research topic due to recent severe global climate changes. In residential buildings, space heating and cooling are the main energy consumers, which are relying on vapor compression-based heat pumps. The HVAC&R industry has moved to phase out refrigerants with high global warming potentials (GWP), e.g., R410A, R22, R134a, R404A, etc. The next-generation refrigerants are mostly mixtures of HFO (Hydrofluoroolefins) refrigerants, e.g., R1234yf and R1234ze(E) combined with the HFC (Hydrofluorocarbons) refrigerant, e.g., R32. Since most of these low-GWP mixtures are in the new A2L lower flammability, research [5] has shown that promoting the use of smaller diameter tubes in heat pump systems is an effective way to reduce refrigerant charge and avoid explosion risk. But it may cause performance degradation.

One characteristic of these low-GWP alternative refrigerants is their high glide, i.e., temperature glides from the bubble point to the dew point at one pressure. High-glide refrigerants prefer multi-row, counter-flow heat exchanger configurations for a single-mode operation. If switching mode, the counter-flow heat exchanger (HX) becomes a parallel-flow heat exchanger. The reversed flow causes significant efficiency degradation. Therefore, improvements in components and system configurations are needed to make the high-glide refrigerants work for both cooling and heating modes to achieve good energy efficiency and protect the environment.

This study demonstrates a low-GWP heat pump design method with a particular focus on the use of a new system configuration for dual-mode reversible heat pumps and 5-mm, 7-mm and 9-mm tube optimized heat exchangers and required modification in compressors. The goals of the study include:

- Investigate the effect of a new system configuration to maintain heat exchanger flow configuration under both cooling and heating modes.
- Optimize multi-row 5-mm, 7-mm, and 9-mm tube coils with low-GWP refrigerants and compressors to determine the performance improvements.
- Analyze the annual performance indices of optimal heat pumps and access their life cycle climate performance (LCCP) to assess carbon footprints.

2. Methodology

2.1. System Model

The DOE/ORNL Heat Pump Design Model (HPDM) [6] is used to model the performance of heat pumps. HPDM is a public-domain HVAC equipment and system modeling and design tool, which supports a free web interface and a desktop version for public use. A finite volume (segment-to-segment) tube-fin HX model is used to simulate the performance of the heat exchanger with different circuitries. This model has been validated by the experimental data [7]. The dehumidification model used in the evaporator simulation is an heat & mass transfer effectiveness-based model [8]. More details of HPDM can be found in [9]. In HPDM, REFPROP 10.0 [10] is used to produce performance look-up tables and simulate the refrigerant properties.

2.2. Selection of Refrigerants

In literature [11], near-term refrigerant candidates have GWP<750 and R32 and R454B can be good drop-in options. Long-term options require GWP<150, and those fluids usually do not match the incumbent fluid (R410A) properties. For fluids with GWP lower than 150 such as R454C, R455A and R457A, they require significant changes in heat exchanger structure to address the high temperaturere glide (temperature rise from the refrigerant bubble point to dew point at constant pressure) and redesign of the compressor to compensate the capacity and efficiency degradation. R1234yf and R1234ze(E) have ultra low GWP values and they are of interest in long term. Table 1 shows the characteristics of R410A and its low-GWP alternatives for a typical residential air source heat pump. The temperature glides are evaluated at saturation pressure corresponding to 8 °C dew-point temperature.

Table 1. Characteristics of refrigerants investigated in this research.

Refrigerant	GWP	Safety Class	Composition: Mass Fraction	Glide in Evaporator [K]	Critical Temperature [°C]
R410A	2088	A1	R32/R125: 50%/50%	0.1	72.8
R32	675	A2L	R32: 100%	0	78.1
R454B	466	A2L	R32/R1234yf: 68.9% /31.3%	1.3	78.1
R454C	146	A2L	R32/R1234yf: 21.5% /78.5%	7.7	85.7
R457A	139	A2L	R32/R1234yf/R152a: 18%/70%/12%	6.9	90.1
R455A	145	A2L	R32/R1234yf/CO_2: 21.5%/75.5%/3%	11.71	85.61
R1234yf	4	A2L	R1234yf: 100%	0	94.7
R1234ze(E)	4	A2L	R1234ze(E): 100%	0	153.7

2.3. Heat Pump System Configuration and Heat Exchanger Structural Parameters

In this study, a 3-ton R410A residential single-stage heat pump product on market is modelled. Fig. 1 shows the schematic of the baseline heat pump operating under cooling mode and heating mode. The refrigerant direction inside the heat exchangers is reversed between mode switching.

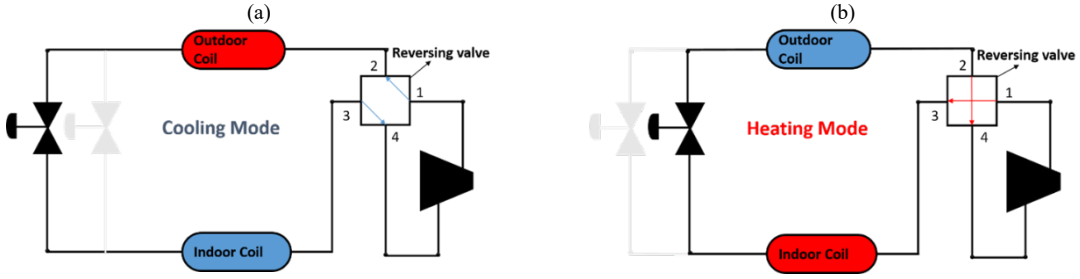

Fig. 1. R410A Baseline Heat Pump System: (a) Cooling Mode Operation; (b) Heating Mode Operation.

To model the baseline system, HPDM has been closely calibrated against experimental data. Table 2 lists the structural parameters of the baseline heat exchangers. The condenser fan moves 2876 CFM of airflow across the outdoor HX and consumes 263 W of power; the indoor blower provides 1205 CFM of supply airflow and consumes 435 W of power. The fan/blower powers and flow rates were the same among all refrigerants.

Table 2. Parameters of Indoor and Outdoor Units of Baseline 3-ton R410A Heat Pump.

Parameters	Indoor HX	Outdoor HX
Coil length [mm]	431.80	2496.82
Coil height [mm]	1248.20	609.60
Coil depth [mm]	35.61	22.00
Number of tubes	120	24
Number of rows	2	1
Number of tubes per row	60	24
Number of circuits	6	3
Circuit pattern (Fig. 2)	cross mixed flow	cross mixed flow
Fin type	Louver fin	Louver fin
Fin density [fins/inch]	16	22
Tube outside diameter [mm]	7.95	9.52
Tube thickness [mm]	0.2794	0.3048
Tube horizontal spacing [mm]	17.81	22.00
Tube vertical spacing [mm]	20.80	25.40

Table 3 lists the empirical correlations used for local heat transfer and pressure drop. For air-to-refrigerant heat exchangers, the thermal resistance is mostly dominated by airside, therefore, it is crucial to model the airside heat transfer coefficient accurately. Different correlations are used according to its suitable application range to improve the prediction of small diameter tube and large diameter tube heat exchangers.

Table 3. Correlations adopted in condenser and evaporator simulations

Operating Mode	Heat Transfer Correlations	Pressure Drop Correlations
Refrigerant - Liquid Phase	Dittus and Boelter (1985) [12]	Blasius (1907) [13]
Refrigerant - Two Phase Boiling (Evaporator)	Thome and Hajal (2003b) [14]	Choi et al. (1999)[15]
Refrigerant - Two Phase Condensation (Condenser)	Cavallini et al. (2006) [16]	Choi et al. (1999) [15]
Refrigerant - Vapor Phase	Dittus and Boelter (1985) [12]	Blasius (1907) [13]
Air	Wang et al. (1999) [17] for 7 & 9-mm tube	Wang et al. (1999) [17] for 7 & 9-mm tube
	Sarpotdar et al. (2016) [18] for 5-mm tube	Sarpotdar et al. (2016) [18] for 5-mm tube

Fig. 2 illustrates 3 typical circuitry patterns by a simple six-tube HX. For the conventional system configuration as used in the baseline system, if the heat exchanger has counter-flow configuration (Fig. 3 (a)) in cooling mode, after the refrigerant flow is reversed in heating mode, the circuitry will become parallel-flow (Fig. 3(c)). And this yields undesirable performance degradation in heating mode.

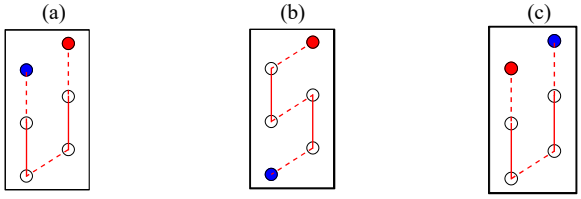

Fig. 2. Heat exchanger circuitry patterns: (a) counterflow, (b) mixed flow, (c) parallel flow

To mitigate the heating performance degradation, the heat exchanger in baseline system is designed as mixed-flow configuration (Fig. 3 (b)) as a compromise solution to balance between cooling and heating modes. The detailed circuitries of the baseline indoor and outdoor heat exchangers are shown in Fig. 3. The indoor HX has 60 tubes per row and 2 tube rows and is divided into 6 mixed flow circuits. The outdoor HX has 24 tubes and 1 tube rows and is divided into 3 circuits. Different colors represent different circuits. The baseline indoor heat exchanger uses 7.95 mm diameter tubes, and the outdoor heat exchanger uses 9.52 mm diameter tubes.

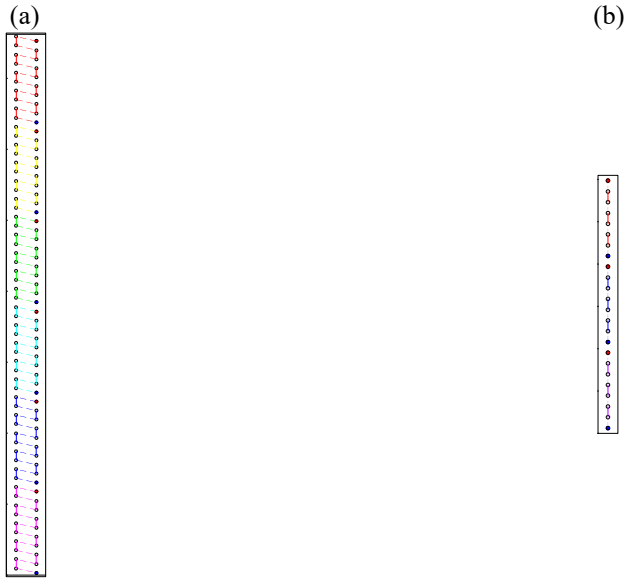

Fig. 3. Baseline tube-fin heat exchanger circuitries: (a) Indoor HX with 7 mm tube; (b) Outdoor HX with 9 mm tube.

As mentioned in the previous section, research has shown that for low-GWP zeotropic mixtures, the counter flow configuration has the most efficient heat transfer performance due to significant saturation temperature glide [5]. With this consideration, one goal of this research is to develop a new system configuration to maintain the same refrigerant flow direction inside the heat exchangers between cooling and heating mode switching. Fig. 4 shows the proposed reversible heat pump system configuration evaluated in the study as the optimized systems. The new configuration has 4 one-way check-valves at the inlet of indoor and outdoor heat exchangers and the heat exchangers have bi-directional distributors. Under both heating and cooling modes, this system configuration can maintain the same heat exchanger circuitry pattern.

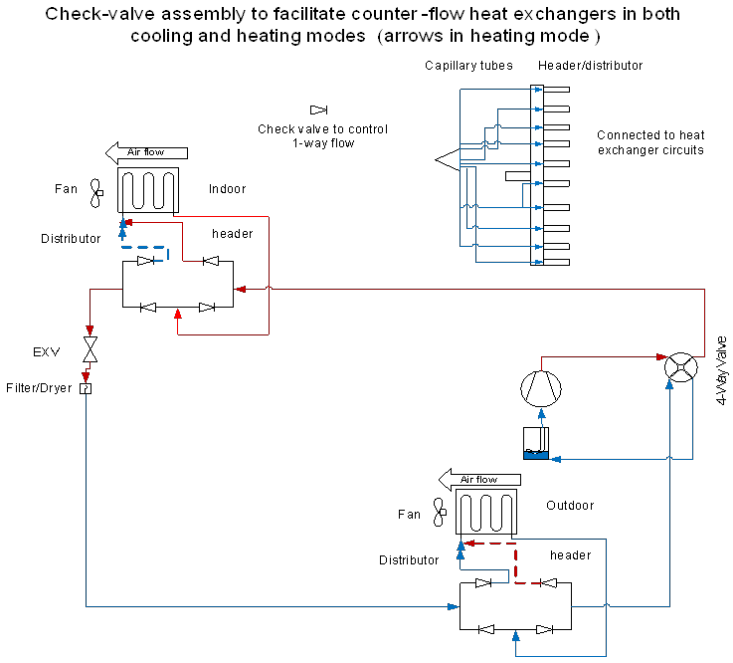

Fig. 4. New System Configuration with Check-valves and Bi-directional distributors Maintaining Counter-flow HXs in Dual Modes

2.4. Optimization Problem Formulation

Shen et al. (2012) [19] developed an optimization framework that integrates HPDM with GenOpt ([20]), a public domain optimization package. In this research, the Particle Swarm Optimization (PSO) algorithm implemented in GenOpt is used to optimize the heat pump system. Regarding PSO setting, the optimization runs use 100 as population size and 200 as number of generations.

Equation (1) shows the optimization problem formulation. The objective is to maximize the Energy Efficient Ratio (EER) of the heat pump under AHRI Standard 210/240 [21] cooling test A condition (95 °F). In Equation (1), the number of circuits for indoor and outdoor heat exchangers are two design variables, which varies between 1 and the number of tubes in each row of the heat exchangers. The number of circuits has a adaptive upper limit to coordinate with the number of tubes in each row.

$$
\begin{aligned}
&\textit{Maximize}: \ EER \\
&\textit{Subject to}: \\
&\quad \textit{Heat exchanger tube diameter} \text{ varies among } 5\ mm, 7\ mm, 9\ mm \\
&\quad 1 \le N_{circuits,evaporator} \le Ntubes\ per\ bank\ of\ evaporator \\
&\quad 1 \le N_{circuits,condenser} \le Ntubes\ per\ bank\ of\ condenser \\
&\quad \Delta T_{superheat,\ evaporator\ outlet} = 10 - \frac{\Delta T_{glide}}{2}\ [R] \\
&\quad 2\ [R] \le \Delta T_{subcooling,\ condenser\ outlet} \le 15\ [R] \\
&\quad Q_{evaporator} = 10.55\ kW \\
&\quad |\ SHR_{evaporator} - SHR_{baseline,evaporator}\ | \ \le 1\% \\
&\quad Height_{evaporator} = Height_{baseline} \\
&\quad Length_{evaporator} = Length_{baseline} \\
&\quad Height_{condenser} = Height_{baseline} \\
&\quad Length_{condenser} = Length_{baseline}
\end{aligned}
\tag{1}
$$

In terms of constraints on operating conditions, the evaporator outlet superheat degree is specified based on the temperature glide of refrigerants as recommended by refrigerant OEM. The condenser outlet subcooling degree is automatically adjusted, but it is constrained between 2 R to 15 R. the cooling capacity of evaporator is a HPDM solving target and set to be the same as the baseline 3-ton R410A heat pump. The compressor displacement volume is altered in HPDM to meet the target evaporator cooling capacity. When modeling the optimized systems using low-GWP refrigerant other than R410A, the compressor isentropic efficiency is fixed as 0.74 and the volumetric efficiency is fixed as 0.98 to be consistent with the baseline R410A system. The goal is to investigate the required displacement volume of the compressor to meet the system capacity for low-GWP refrigerants.

In terms of constraints on heat exchanger dimensions, the last four constraints in Equation (1) guarantee that the optimized indoor and outdoor heat exchangers have the same frontal shapes as the baseline heat exchangers, i.e., the optimal heat exchangers can fit into the original indoor and outdoor fan-coil unit perfectly. This can ease the retrofit effort of upgrading the R410A heat pump to the new low-GWP system by minimizing the change in manufacturing and installation processes and guarantee that the optimized systems have the best compatibility with end-users' house structure. As a result, the new products can be easily accepted by manufacturers and end-users.

The staggered tube layout and tube spacing for 5-mm, 7-mm and 9-mm tubes used in the optimized coils are shown in Fig. 5. These tube layout and spacings are off-the-shelf designs from a heat exchanger manufacturer. The heat exchanger circuitry pattern is fixed as counter flow configuration, since counter-flow pattern has the most efficient heat transfer for high-glide zeotropic mixtures [5].

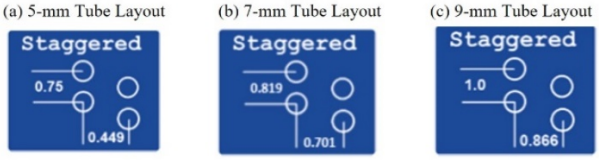

Fig. 5. Horizontal spacing and vertical spacing in inch for (a) 5-mm tube HX; (b) 7-mm tube HX; (c) 9-mm tube HX.

3. Results

3.1. Drop-in Performances

Without modification of the system configuration and components, Fig. 6 shows the drop-in performance for cooling operation at 95 °F. In terms of capacity (Fig. 6 (a)), R32 induces a capacity increase by 8.3% and R454B shows 1.48% capacity decrease compared with the R410A baseline. If the baseline R410A heat exchangers and compressor are used, R454C, R455A, R457A, R1234yf and R1234ze(E) induce 29.4%, 26.8%, 32.9%, 46.9% and 55.5% capacity degradation, respectively, without changing any component.

In terms of EER, the variation is very small. R32, R454B, R457A and R1234yf induces EER increases by 2.2%, 3.2%, 1% and 3.3%, while R454C, R455A and R1234ze(E) and induces EER decreases by 0.7%, 2.6% and 0.4%, respectively.

For the drop-in test, the compressor isentropic efficiency and volumetric efficiency are predicted by 10-coefficient compressor map provided by the compressor manufacturer. Despite the compressor map is regressed for R410A test data, a scaling method assuming the same isentropic and volumetric efficiencies at the same suction and discharge saturation temperatures for R410A is used to predict the compressor performance when other refrigerants are used. This compressor scaling method is validated against experiment data [11] and demonstrates good prediction accuracy.

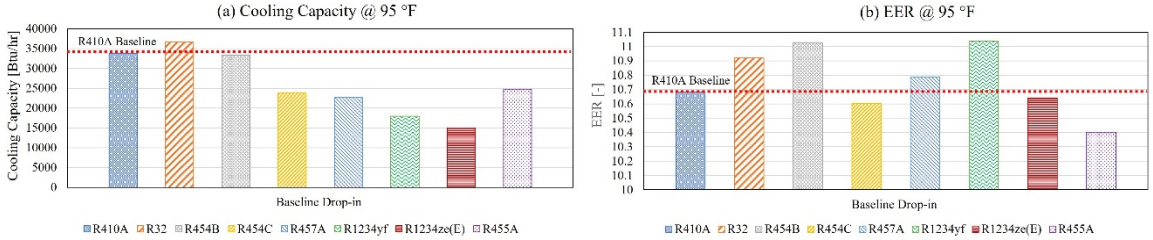

Fig. 6. Baseline System Drop-in Cooling Performance at 95 °F (a) Cooling Capacity; (b) EER

Similar as the cooling performance, Fig. 7 shows the drop-in performance for heating operation under AHRI 210/240 heating C_1 condition at 47 °F. R32 shows a 6.7% capacity increase and 0.03% COP increase. R454B

shows comparable performance to R410A, i.e., a 3.9% capacity decrease and 1.72% COP increases. R454C, R455A, R457A, R1234yf, R1234ze and induces 6.5%, 27.6%, 38.9%, 52.3% and 62.5% capacity degradation, respectively.

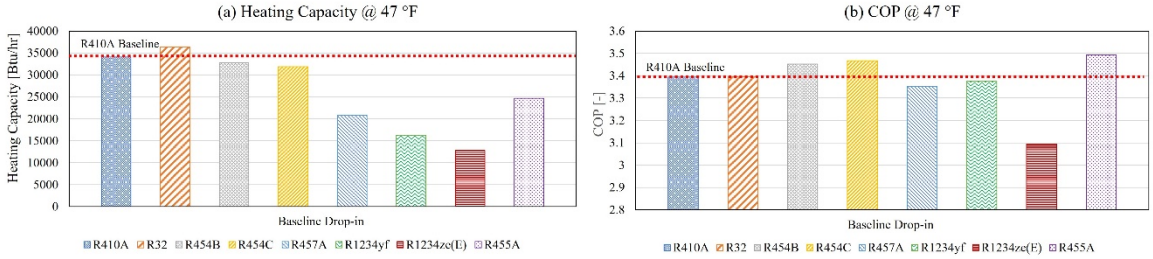

Fig. 7. Baseline System Drop-in Heating Performance at 47 °F (a) Heating Capacity; (b) COP

As a conclusion, these results show that R32 and R454B are good drop-in candidates. However, GWP<150 refrigerants cannot be directly drop-in due to the significant capacity degradation. For low-GWP refrigerants, it is necessary to redesign the system configuration and components to meet the performance metrics. One required change for the compressor is to increase the displacement volume to increase capacity.

3.2. Optimization Results

The previous section shows the drop-in test results, which demonstrates the system efficiency and capacity degrade with drop-in of low-GWP refrigerants. This section shows the results after conducting design optimization of the components and adopting the new system configuration. For all optimization cases, the suction line is sized such that the saturation temperature drop of the suction line for different refrigerants is the same as that of the baseline R410A system. The goal is to investigate the required displacement volume of the compressor to match the R410A system capacity and efficiency requirements.

All cooling-optimized systems using 5-mm, 7-mm and 9-mm tube heat exchangers satisfy the cooling capacity requirements (i.e., 36000 BTU/hr) to match the baseline 3-ton unit. Fig. 8 shows the cooling performance comparison at 95 °F. For R410A, R32, R454B, R455A and R457A, the optimized 5-mm tube heat exchangers yield 9.4%, 11.6%, 9.4%, 5.5% and 5.1% EER improvements, respectively. Except R32 and R454B, using 7-mm tube and 9-mm tube with GWP less than 150 refrigerants yields performance degradation compared with the baseline drop-in test. For refrigerants with GWP less than 150, heat exchanger design optimization does not show efficacy to improve system performance. In this study, the advantage of using 5 mm tube HXs attributes to the increased heat transfer area and reduced mass flux in each circuit as shown in Table 4. Despite the optimized heat exchangers have the same coil width and coil height as the baseline coils, 5-mm tube heat exchangers consist of more tubes in each row and more tube rows due to smaller horizonal and vertical tube spacing as shown in Fig. 5.

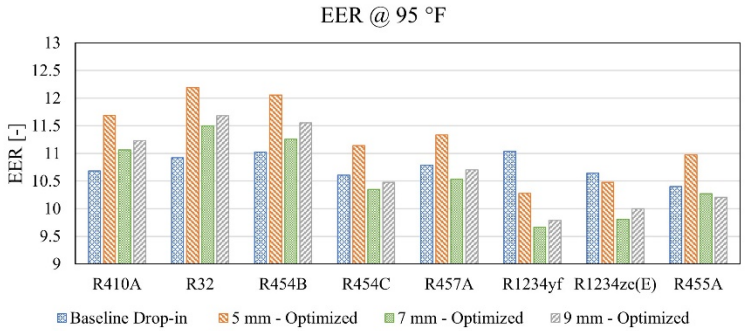

Fig. 8. Cooling Performance Comparison of Baseline and Optimal Systems at 95 °F (a) Cooling Capacity; (b) EER

The cooling optimized designs are evaluated under heating mode at 47 °F. Their performances are depicted in Fig. 9. As shown in Fig. 9(a), the optimal systems using most refrigerants fluids can satisfy the heating capacity of R410A baseline, except R1234ze(E) which induces significant capacity degradation.

In terms of COP (Fig. 9(b)), systems using 5-mm tube optimized heat exchangers show the most performance improvements, i.e., 11.4%, 12.7%, 10.2%, 0.05%, 1.2%, 6.3%, 1.0% and 10.0% for R410A, R32, R454B, R455A, R457A, R1234yf and R1234ze(E), respectively. The performance of optimized 7-mm tube

HX is close to the baseline system and the performances of system using 9-mm tube HXs are better than the baseline for R32, R454B, R454C, R457A and R1234ze(E), but worse than the baseline for R455A and R1234yf.

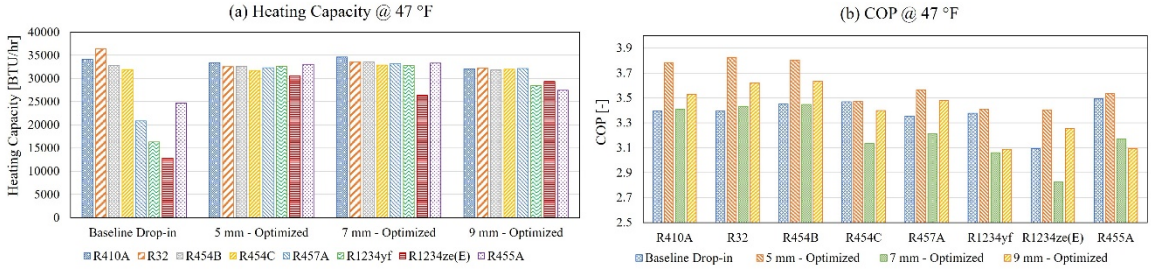

Fig. 9. Heating Performance Comparison of Baseline and Optimal Systems at 47 °F (a) Heating Capacity; (b) COP

Fig.10 (a) shows the refrigerant charge of the optimized systems. Use of 5-mm tube heat exchanger yields charge reduction. The charge reductions range from 28.4% to 43.7%. While 7-mm tube heat exchangers increase the system charge, and 9-mm tube heat exchangers have the comparable charge amount compared with the baseline system.

Fig.10 (b) shows the redesigned compressor displacement volumes for each refrigerant to match the baseline cooling capacity. The required compressor displacement volume is not sensitive to the tube diameters used in the heat exchanger, rather, it is sensitive to the property of fluids. In general, R32 induces displacement volume decreases by 15.8% while R454B, R455A, R457A, R1234yf and R1234ze(E) induce increased displacement volume increases by 4.7%, 40.2%, 50.7%, 62.2%, 152.6% and 224.2%. These results demonstrate the importance of compressor redesign for low-GWP heat pumps. In general, systems using low-GWP refrigerants require larger compressors than systems using R410A.

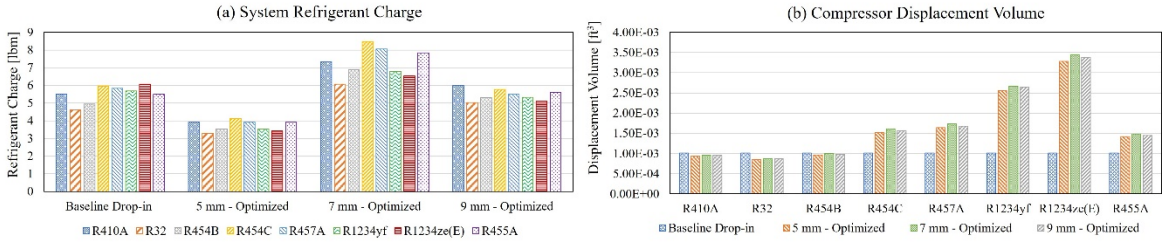

Fig.10. (a) System Refrigerant Charge; (b) Designed Compressor Displacement Volume.

To access the annual performance of optimized systems. The seasonal energy efficiency ratio-2 (SEER2) and heating seasonal performance factor-2 (HSPF2) are calculated according to AHRI 210/240 test standards [21]. Effective January 1st, 2023, SEER2 and HSPF-2 are used to rate system performance following a more stringent testing procedure. The new testing procedure increases the systems' external static pressure by a factor of five to better reflect field conditions of installed equipment in a typical ducted system and results in a lower numerical rating value for the same product. The performance degradation owing to frost accumulation has been considered by applying performance degradation factors, i.e., 0.91 for heating capacity and 0.985 for power consumption at the 35˚F dry bulb/33˚F wet bulb frosting condition.

From Fig. 11 (a), the SEER2 of the baseline R410A system is 11.42. R32 and R454B optimized coils can satisfy the baseline SEER2 criteria. Among the five GWP less than 150 refrigerants, the three fluids which overperform baseline is R454C, R457A and R455A using 5-mm tube heat exchangers. The optimized system using R1234yf and R1234ze(E) shows smaller SEER2 after dimension-constrained heat exchanger optimization and compressor sizing.

Fig. 11 (b) shows the HSPF2 of the baseline and optimal systems. The HSPF2 of the baseline R410A system is 7.17. R32 and R454B can satisfy the HSPF requirement regardless of the choice of heat exchanger tubes. When using 5-mm tube heat exchangers with GWP<150 refrigerants, HSPF2 of the optimized systems exceeds HSPF2 of the baseline.

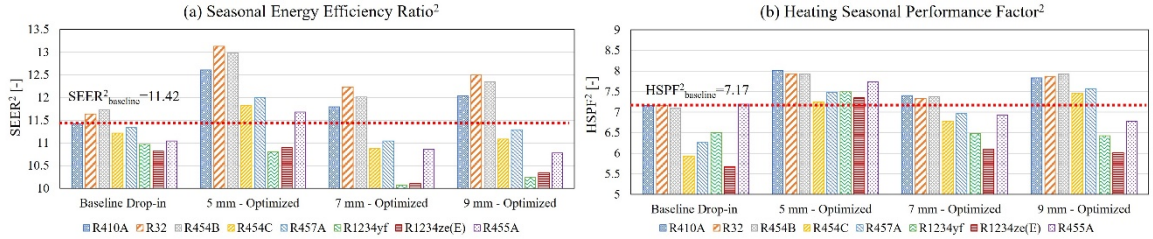

Fig. 11. Heat Pump Systems Performance Comparison (a) Seasonal Energy Efficiency Ratio; (b) Heating Seasonal Performance Factor

To streamline the performance of different heat exchangers with different low-GWP refrigerants, the SEER2 and HSPF2 are shown in Fig. 12. The marker shapes represents different system types, i.e., either the baseline system or optimal systems with different diameter tubes. And the marker colors show different refrigerants. The performance of the baseline R410A system (SEER2-11.4/HSPF2-7.2) is highlighted as the cross in the center . By comparing the baseline performance with optimized systems, the design space is divided into 4 regions. The system designs located in the upper right region has both cooling and heating performance superior to the baseline and the system designs located in the bottom left region has dual-mode performance inferior to the baseline. The other two regions have designs with only 1 mode better than the baseline. In the upper right region. The best performances are achieved using R32 (SEER2-13.1/HSPF2-7.9), followed by R454B (SEER2-13.0/HSPF2-7.9) and R410A (SEER2-12.6/HSPF2-8.0). For the GWP <150 fluids, three design candidates using R457A (SEER2-12.0/HSPF2-7.5), R454C (SEER2-11.8/HSPF2-7.2) and R455A (SEER2-11.7/HSPF2-7.7) satisfy both heating and cooling performance requirements.

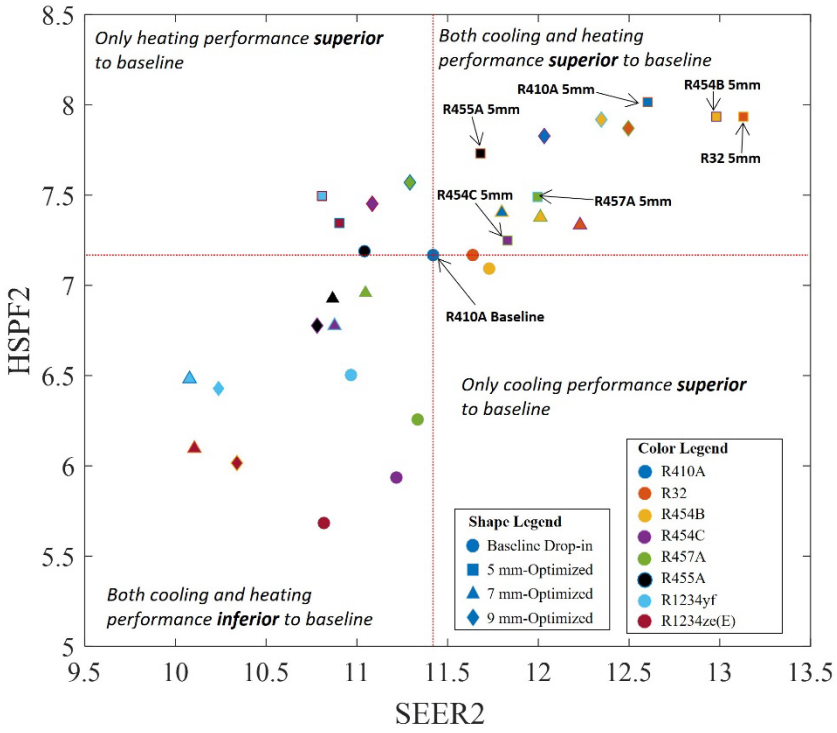

Fig. 12. SEER2 and HSPF2 of Baseline Drop-in Tests and Optimized Systems

Table 4 shows the heat exchanger structures for those optimal systems in Fig. 12. For brevity, the heat exchanger structure is denoted as *Number of Tubes per Row* x *Number of Rows* - *Number of circuits*. For example, the 7-mm tube indoor baseline heat exchanger in Fig. 3 has 60 tubes per row, 2 rows and has 6 circuits, so its structure is 60x2-6, and the 9-mm tube outdoor baseline heat exchanger has 24 tubes per row, 1 row and 3 circuits, so its structure is 24x1-3. Following this convention, the heat exchanger structures of the optimized system are listed in Table 4.

Table 4. Heat Exchanger Structure of Optimized Systems

HX Structure	5 mm - Optimized		7 mm - Optimized		9 mm - Optimized	
	Indoor HX	**Outdoor HX**	**Indoor HX**	**Outdoor HX**	**Indoor HX**	**Outdoor HX**
R410A	64x3-16	32x2-16	60x2-6	30x2-6	48x2-6	24x1-2
R32	64x3-16	32x2-16	60x2-6	30x2-5	48x2-6	24x1-2
R454B	64x3-16	32x2-16	60x2-6	30x2-10	48x2-4	24x1-2
R454C	64x3-32	32x2-16	60x2-12	30x2-6	48x2-6	24x1-3
R457A	64x3-32	32x2-16	60x2-12	30x2-6	48x2-6	24x1-3
R455A	64x3-32	32x2-16	60x2-15	30x2-6	48x2-8	24x1-3
R1234yf	64x3-32	32x2-16	60x2-15	30x2-6	48x2-8	24x1-3
R1234ze(E)	64x3-32	32x2-16	60x2-15	30x2-6	48x2-8	24x1-3

From Table 4, the optimal 5-mm tube indoor HX has two structures depending on the fluids, either 64x3-16 or 64x3-32. The optimal 5-mm tube outdoor HXs regardless of fluids have the same structure, i.e., 32x2-16. Compared with the baseline indoor 7-mm tube HX (60x2-6) and baseline outdoor 9-mm tube HX (24x1-3), the number of circuits are significantly increased for optimal HXs using 5-mm tube. The optimizer increases number of circuits to distribute refrigerant mass flow such that the refrigerant pressure drop in the heat exchangers can be reduced and the effect caused by the decreased tube cross sectional area is mitigated.

3.3. Life cycle climate performance analysis

To understand the environmental impacts of optimized heat pumps using the new system configuration and the optimal HX structures with low-GWP refrigerants, life cycle climate performance (LCCP) evaluation is used to analyze the direct and indirect greenhouse gas (GHG) emissions of the system over the course of its lifetime from manufacturing to disposal. It is calculated as the sum of direct and indirect emissions generated over the lifetime of the system "from cradle to grave". Direct emissions include all effects from the release of refrigerant into the atmosphere during the lifetime of the system. Direct emissions include:

- Annual refrigerant loss from gradual leaks
- Losses at the end-of-life disposal of the unit
- Large losses during operation of the unit
- Atmospheric reaction products from the breakdown of the refrigerant in the atmosphere

The indirect emissions include:

- Emissions from electricity generation
- Emission from the manufacturing of materials
- Emissions from the manufacturing of refrigerants
- Emissions from the disposal of the unit

More details about LCCP evaluation method can be referred to Wan et al. (2021) [22]. The input values used for evaluating the LCCP are shown in Table 5 including the cut-off outdoor temperature and the temperature at which the heat pump starts. A critical part of the LCCP is the assumed leak rate and end of life recovery. 2% leak rate per year with 18 years lifetime and 20% end of life recovery are specified based on ASHRAE 189.1. To compare systems using different low-GWP refrigerants, Chicago is selected for a case study and its TMY-3 weather data is used for annual performance evaluation.

Table 5. Input Values for Baseline and Optimal Systems LCCP Evaluation

Factor	Value
Refrigerant	R-410A or its alternatives
Refrigerant charge (kg)	As shown in Fig. 10 (a)
Unit weight (kg)	190
Annual refrigerant leakage (%)	2
EOL leakage (%)	80
Lifetime (years)	18
Cut-off temperature (°C)	−17.8
Temperature at which the heat pump starts (°C)	−12.2
Weather data	Chicago TMY-3

Fig.13 shows the comparison of the direct and indirect emissions for systems. Compared to R410A baseline, systems using other refrigerants reduce direct emissions as shown in Fig.13 (a). This attributes to their lower GWP value and the reduced system charge as shown in Fig. 10 (a).

Fig.13 (b) shows the comparison of the indirect emissions. The optimized systems have 10%-16% lower indirect emissions than the baseline system due to the improved EER (Fig.13 (a)) and improved COP (Fig.

14). The 5-mm optimal designs with R454C and R457A induces significant indirect emission reductions. This indirect emission reduction attributes to improved SEER2 and HSPF2 as shown in Fig. 11 and Fig. 12. Since Chicago is a city in the heating climate region IV with both significant number of heating and cooling days, the indirect emissions are affected by both cooling and heating performance.

It is worthwhile to mention that the reduction potential is different in another climate zone. For example, in a location with warm or mild climate, the SEER2, i.e., the cooling efficiency plays a more dominant role since the heat pump is mostly operated in cooling mode.

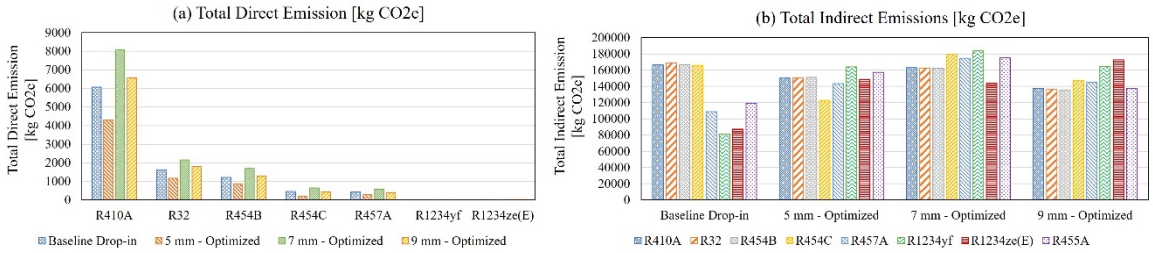

Fig.15. Greenhouse gas emissions of the baseline and low-GWP optimized systems (a) Direct Emission; (b) Indirect Emission.

Fig. 14 shows the comparison of the total emissions. In fact, 96%-98% of the total emission is comprised of indirect emissions. So indirect emission dominates the total emission. Although many designs using 7-mm tube and 9-mm tube heat exchangers show great emission reduction potential, they cannot meet the cooling and heating efficiency requirements as shown in Fig. 12. The three feasible designs satisfying the efficiency requirements are systems using 5-mm tube heat exchangers with R454C, R455A and R457A. The optimal 5-mm tube systems using R454C, R455A and R457A yields 28.6%, 8.5% and 16.5% lifetime emission reduction compared to the baseline R410A system.

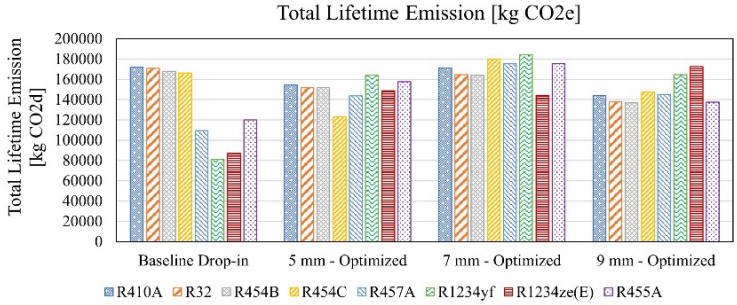

Fig. 16. Total greenhouse gas emissions of the baseline and low-GWP optimized systems.

4. Conclusion

This study presents heat exchanger and system development technologies to support the transition to refrigerants with GWP lower than 150. Higher than baseline R410A system efficiency levels in cooling and heating modes are achieved by a model-based design optimization approach based on simulation using detailed hardware information. The new reversible heat pump systems with low-GWP refrigerants adopt a new system configuration, the optimized indoor and outdoor heat exchangers, an optimized compressor. The potential of 5-mm, 7-mm and 9-mm tube in heat exchangers are investigated. The optimal systems using R454C, R455A and R457A with 5-mm tube heat exchangers outperform the baseline R410A heat pump product. Life cycle climate analysis shows that the optimized systems using GWP lower than 150 fluids reduce the lifetime CO_2 emissions by 8.5%-28.6%, while guaranteeing the same or better capacity and efficiency performance than the baseline.

The optimal heat exchanger designs obtained from this research can fit into the original R410A heat exchanger ducts and chasses, which helps to minimize changes in manufacturing and installation. As a result, the system retrofit impacts on manufacturers and end users are minimized. The proposed design approach establishes a production and installation path to produce cost-effective high-performance low GWP reversible heat pumps.

Acknowledgments

The research used resources at the Building Technologies Research and Integration Center, a DOE Office of Science User Facility operated by the Oak Ridge National Laboratory. The authors would like to acknowledge Antonia Bouza, the DOE Building Technologies Office technology manager for his support.

References

1. Coulomb, D., J. Dupont, and V. Morlet, *The impact of the refrigeration sector on the climate change. 35th Informatory Note on Refrigeration Technologies.* Paris (France), 2017.
2. Schulz, M. and D. Kourkoulas, *Regulation (EU) No 517/2014 of The European Parliament and of the council of 16 April 2014 on fluorinated greenhouse gases and repealing Regulation (EC) No 842/2006.* Off. J. Eur. Union, 2014. **2014**(517): p. L150.
3. Clark, E. and S. Wagner, *The Kigali Amendment to the Montreal Protocol: HFC Phase-Down.* Ozon Action UN Environment (UNEP), 2016: p. 1-7.
4. Agreement, P. *Paris agreement*. in *Report of the Conference of the Parties to the United Nations Framework Convention on Climate Change (21st Session, 2015: Paris). Retrived December*. 2015. HeinOnline.
5. Li, Z., B. Shen, and K.R. Gluesenkamp, *Multi-objective optimization of low-GWP mixture composition and heat exchanger circuitry configuration for improved system performance and reduced refrigerant flammability.* International Journal of Refrigeration, 2021. **126**: p. 133-142.
6. Shen, B. and K. Rice, *DOE/ORNL heat pump design model.* Web link: http://hpdmflex. ornl. gov, 2016.
7. Abdelaziz, O., et al., *Alternative Refrigerant Evaluation for High-Ambient-Temperature Environments: R-22 and R-410A Alternatives for Rooftop Air Conditioners.* Energy and Transportation Science Division. Oak Ridge National Laboratory. ORNL/TM-2016/513, 2016.
8. Braun, J., S. Klein, and J. Mitchell, *Effictiveness models for cooling towers and cooling coils.* ASHRAE Transactions (American Society of Heating, Refrigerating and Air-Conditioning Engineers);(USA), 1989. **95**(CONF-890609--).
9. Shen, B., et al., *Model-based optimizations of packaged rooftop air conditioners using low global warming potential refrigerants.* International Journal of Refrigeration, 2018. **87**: p. 106-117.
10. Lemmon, E.W., M.L. Huber, and M.O. McLinden, *NIST standard reference database 23.* Reference fluid thermodynamic and transport properties (REFPROP), version, 2010. **9**.
11. Shen, B., Z. Li, and K.R. Gluesenkamp, *Experimental study of R452B and R454B as drop-in replacement for R410A in split heat pumps having tube-fin and microchannel heat exchangers.* Applied Thermal Engineering, 2022. **204**: p. 117930.
12. Dittus, F. and L. Boelter, *Heat transfer in automobile radiators of the tubular type.* International Communications in Heat and Mass Transfer, 1985. **12**(1): p. 3-22.
13. Blasius, H., *Grenzschichten in Flüssigkeiten mit kleiner Reibung*. 1907: Druck von BG Teubner.
14. Thome, J.R. and J.E. Hajal, *Two-phase flow pattern map for evaporation in horizontal tubes: latest version.* Heat Transfer Engineering, 2003. **24**(6): p. 3-10.
15. Choi, J.-Y., M.A. Kedzierski, and P. Domanski, *A generalized pressure drop correlation for evaporation and condensation of alternative refrigerants in smooth and micro-fin tubes*. 1999: US Department of Commerce, Technology Administration, National Institute of ….
16. Cavallini, A., et al., *Condensation in horizontal smooth tubes: a new heat transfer model for heat exchanger design.* Heat Transfer Engineering, 2006. **27**(8): p. 31-38.
17. Wang, C.-C., et al., *Heat transfer and friction correlation for compact louvered fin-and-tube heat exchangers.* International journal of heat and mass transfer, 1999. **42**(11): p. 1945-1956.
18. Sarpotdar, S., D. Nasuta, and V. Aute, *CFD Based Comparison of Slit Fin and Louver Fin Performance for Small Diameter (3mm to 5 mm) Heat Exchangers.* 2016.
19. Shen, B., O. Abdelaziz, and K. Rice, *Auto-calibration and control strategy determination for a variable-speed heat pump water heater using optimization.* HVAC&R Research, 2012. **18**(5): p. 904-914.
20. Wetter, M. *GenOpt-A generic optimization program*. in *Seventh International IBPSA Conference, Rio de Janeiro*. 2001.
21. AHRI, A., *Standard 210/240-2008.* Performance Rating of Unitary Air Conditioning and Air-Source Heat Pump Equipment, AHRI, Ed, 2008.
22. Wan, H., et al., *A comprehensive review of life cycle climate performance (LCCP) for air conditioning systems.* International Journal of Refrigeration, 2021. **130**: p. 187-198.